CHAPTER FOUR

Iron–Sulfur Clusters in Zinc Finger Proteins

Geoffrey D. Shimberg[2], Jordan D. Pritts[2], Sarah L.J. Michel[1]
School of Pharmacy, University of Maryland, Baltimore, MD, United States
[1]Corresponding author: e-mail address: smichel@rx.umaryland.edu

Contents

Abstract

Zinc finger (ZF) proteins are proteins that use zinc as a structural cofactor. The common feature among all ZFs is that they contain repeats of four cysteine and/or histidine residues within their primary amino acid sequence. With the explosion of genome sequencing in the early 2000s, a large number of proteins were annotated as ZFs based solely upon amino acid sequence. As these proteins began to be characterized

[2] G.S. and J.P. contributed equally to this work.

Methods in Enzymology, Volume 599
ISSN 0076-6879
https://doi.org/10.1016/bs.mie.2017.09.005

experimentally, it was discovered that some of these proteins contain iron–sulfur sites either in place of or in addition to zinc. Here, we describe methods to isolate and characterize one such ZF protein, cleavage and polyadenylation specificity factor 30 (CPSF3O) with respect to its metal-loading and RNA-binding activity.

1. INTRODUCTION

Zinc fingers (ZFs) are a large family of principally eukaryotic proteins that utilize zinc as a cofactor to fold and function (Jantz, Amann, Gatto, & Berg, 2004; Lee & Michel, 2014; Maret, 2012; Michalek, Besold, & Michel, 2011). ZFs contain repeats of four invariant cysteine and/or histidine residues within their primary amino acid sequences, and these residues serve as ligands for the Zn^{2+} ion (Lee & Michel, 2014; Michalek et al., 2011). Although first identified in the 1980s, the ubiquity of ZFs was not fully appreciated until the late 1990s/early 2000s with the advent of whole-genome sequencing (Andreini, Banci, Bertini, & Rosato, 2006; Berg, 1986, 1988; Bertini, Decaria, & Rosato, 2010; Decaria, Bertini, & Williams, 2010; Laity, Lee, & Wright, 2001). From these sequencing efforts, between 3% and 10% of all proteins were annotated as ZFs, based upon the presence of cysteine/histidine-rich sequences (Lee & Michel, 2014). These ZFs have been separated into different classes, with ZFs grouped based upon the number and spacing of cysteine and histidine residues within each ZF domain (Krishna, Majumdar, & Grishin, 2003; Lee & Michel, 2014; Magyar & Godwin, 2003; Matthews & Sunde, 2002; Michalek et al., 2011). Presently, at least 14 classes of ZFs have been defined.

Most of the ZFs that have been identified from genome sequencing have not yet been studied experimentally; therefore, in many cases whether these "zinc finger" proteins are bona fide zinc fingers is not known. In the last few years, several proteins annotated as "zinc fingers" have been found to harbor iron–sulfur clusters, in lieu of or in addition to zinc. The first of these proteins to be identified was mitoNEET, which contains a 3-cysteine, 1-histidine (CCCH) motif within its primary sequence (Baxter, Jennings, & Onuchic, 2012; Conlan et al., 2009; Tamir et al., 2015; Wiley, Murphy, Ross, van der Geer, & Dixon, 2007; Wiley, Paddock, et al., 2007). MitoNEET attracted initial interest because it was found to be a target of the antidiabetes drug pioglitazone (Colca et al., 2004). Subsequently, mitoNEET was found to play a key role in electron transport, and there is emerging evidence for roles in iron regulation, mitochondrial energy metabolism, and Fe–S cluster regulation

(Lipper et al., 2015; Wang, Landry, & Ding, 2017). Despite being annotated as a "zinc finger" because it contains a conserved CCCH domain that is typically related to zinc binding, mitoNEET turned red upon protein expression and purification and was found to contain a 2Fe–2S cluster, coordinated to the CCCH "zinc finger" ligands (Wiley, Paddock, et al., 2007) (Fig. 1). Subsequently, two close homologs of mitoNEET, Miner1 and Miner2, were also shown to contain 2Fe–2S clusters bound to their CCCH motifs (Conlan et al., 2009; Lin, Zhang, Lai, & Ye, 2011). In addition, 2Fe–2S clusters were identified in the *Escherichia coli* iron–sulfur cluster assembly proteins IscR and IscU and the yeast Grx3/4/Fra2-signaling proteins (Blanc, Gerez, & Ollagnier de Choudens, 2015; Li et al., 2009). These findings brought into question the dogma that proteins with conserved cysteine/histidine sequences are *always* ZFs; moreover, this underscores the need for experimental validation of the metal identity and coordination.

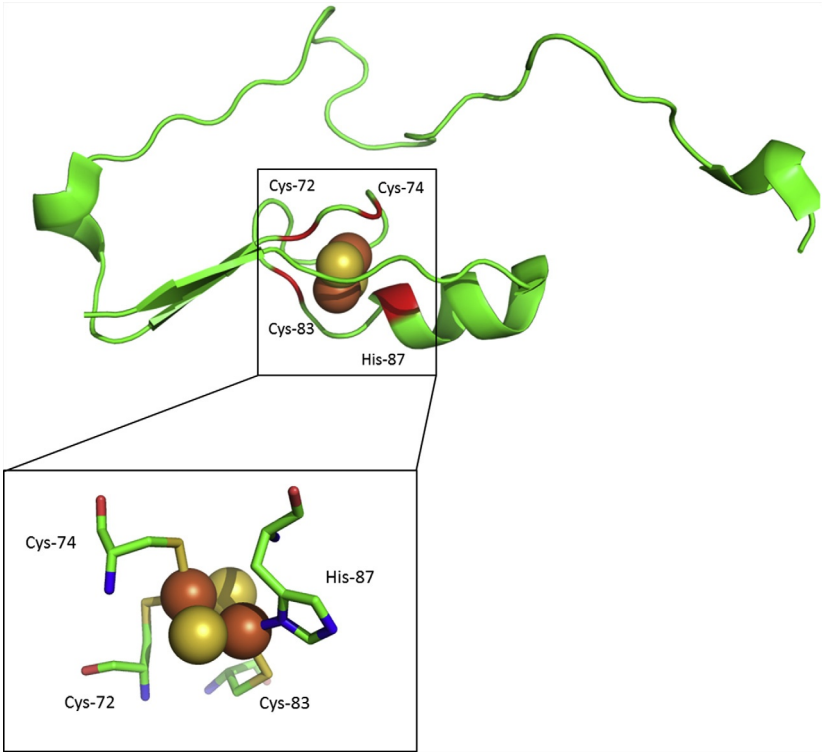

Fig. 1 Structure of mitoNEET with the 2Fe–2S cluster highlighted (PDB 2R13, figure made in PyMol).

More recently, our laboratory identified another intriguing eukaryotic protein annotated as a ZF that contains a 2Fe–2S cluster (as initially observed as a reddish colored protein) (Figs. 2 and 3A). This protein, cleavage and polyadenylation specificity factor 30 (CPSF30) contains five CCCH domains and is a hybrid of an iron–sulfur cluster/ZF protein (Shimberg et al., 2016). CPSF30 houses a 2Fe–2S cluster with one CCCH ligand set, analogous to mitoNEET, Miner1 and Miner2, and four zinc-loaded CCCH ZF sites, analogous to traditional ZFs (Shimberg et al., 2016). (Fig. 2) The full biological role of CPSF30 is not yet understood; however, it is known to be involved in pre-mRNA regulation. We have shown that CPSF30 binds the AU-rich hexamer of RNA present in the majority of pre-mRNA molecules (Yang & Doublie, 2011) by measuring protein/RNA binding with a synthetic RNA sequence that corresponds to α-synuclein pre-RNA. The interaction is sequence selective and requires that both iron and zinc sites be present (Shimberg et al., 2016). As this hexamer is conserved in approximately 90% of pre-mRNA molecules (Beaudoing, Freir,

ZF1	S	G	A	A	V	C	E	F	F	L	K	A	A	–	C	G	K	G	G	M	C	P	F	R	H	I	S	G
ZF2		K	T	V	V	C	K	H	W	L	R	G	L	–	C	K	K	G	D	Q	C	E	F	L	H	E	Y	D
ZF3	T	K	M	P	E	C	Y	F	Y	S	K	F	G	E	C	S	N	K	E		C	P	F	L	H	I	D	P
ZF4	S	K	I	K	D	C	P	W	Y	D	R	G	F	–	C	K	H	G	P	L	C	R	H	R	H	T	R	R
ZF5					I	C	V	N	Y	L	V	G	F	–	C	P	E	G	P	S	C	K	F	M	H	P	R	F

Fig. 2 Sequence alignment of the CPSF30 CCCH domains.

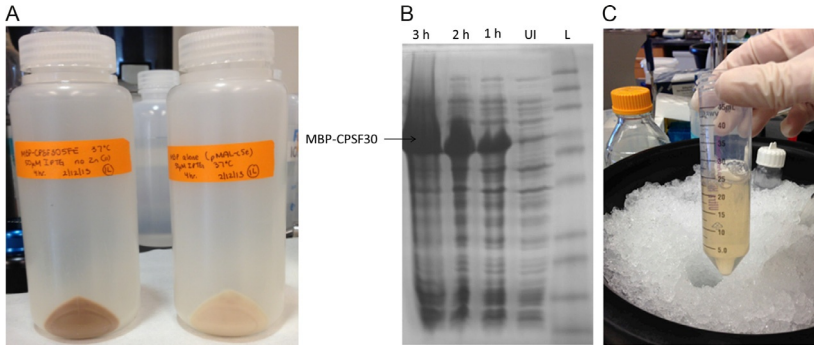

Fig. 3 The induction through sonication of CPSF30. (A) Comparison of CPSF30 (*left*) cell paste vs MBP (*right*), postoverexpression. CPSF30 results in a rust-colored protein sample indicative of the presence of an iron cofactor. (B) 15% SDS-PAGE of CPSF30 protein induction trial. From right to left is the Invitrogen BenchMark Protein Ladder (Thermo Fisher), uninduced pellet, and induced pellet after 1, 2, and 3 h. (C) Image of the soluble fraction of CPSF30 after sonication of the CPSF30 pellet. Note that the protein retains the *reddish hue*.

Wyatt, Claverie, & Gautheret, 2000), it can be inferred that CPSF30 has a broad application to bind various pre-mRNA sequences aiding polyadenylation. In this chapter, we describe the methods we utilize to isolate metal-loaded CPSF30 and assess its RNA-binding activity. Our approach utilizes established methods used to isolate traditional ZF proteins combined with those for Fe–S proteins. This approach has the potential to be utilized for the isolation and analysis of other ZF proteins that have been identified from genome sequences, but not yet characterized experimentally.

2. APPROACHES TO CLONE ZINC FINGER/Fe–S CLUSTER GENES

2.1 Cloning Strategy

When choosing the expression system for a ZF and/or Fe–S protein, like most proteins, a wealth of options are commercially available. Choosing an appropriate vector is critical to ensure that proper protein production is successful. The expression of proteins containing ZFs as well as ZFs with Fe–S clusters is often achieved using commercial pET vectors (example: pET-28a, Novagen, Cat. No. 69864-3) containing either C- or N-terminal hexahistidine tags (his-tag). This is an effective method when the protein is inherently soluble (Woestenenk, Hammarström, van den Berg, Härd, & Berglund, 2004) and there are multiple examples of the use of a hexahistidine tag to purify a protein with an Fe–S cluster, with some recent examples in these references (Boal et al., 2005; Engstrom, Partington, & David, 2012; Poor et al., 2014; Tan et al., 2012) as well as for ZFs. We note that in some cases, if the metal site is labile, the use of this approach may disrupt native metal binding and therefore should be considered on a case-by-case basis (Zhao & Huang, 2016). As an example, the pET-28a expression system contains an N-terminal his-tag, thrombin cleavage site, T7 tag, and an optional C-terminal his-tag. Upon protein overexpression, purification is accomplished via immobilized metal affinity chromatography (IMAC), in which the hexahistidine tag binds to nickel (cobalt, copper, or iron)-loaded resin in the solid phase (Persikov & Singh, 2014). The protein of interest can then be eluted and separated from other cellular proteins using an imidazole buffer gradient. The T7 tag can be utilized for further purification of the protein of interest if needed. Incorporation of a thrombin cut site allows cleavage of the N-terminal his-tag yielding native protein postpurification. Determination of whether to utilize a C- vs N-terminal his-tag is accomplished empirically—proteins with either

tag appended are produced and the resultant protein's stability, solubility, and activity are assessed. N-terminal his-tags are generally more common, as cloning design and gene insertion into the vector is more straightforward (see, for example, Boal et al., 2005). We note that for some iron–sulfur proteins, a C-terminal hexahistidine tag has proven more robust, as seen with RimO (Lee et al., 2009). If the protein of interest contains an Fe–S cluster near the far end of the N-terminus, a C-terminal tag may be preferred as there is concern that the hexahistidine residues may alter the Fe-binding properties at the Fe–S ligand site (Lanz et al., 2012). The pET-28a expression system also contains kanamycin resistance allowing bacterial selection containing the plasmid (Pattenden & Thomas, 2008). These expression systems are well suited for small ZFs with moderate to high solubility.

Where native protein solubility is a concern, particularly for larger ZF proteins, we and other laboratories have found that the utilization of a vector that encodes for a maltose-binding protein (MBP) tag [e.g., pMAL-c5E (discontinued), pMAL-c5X or pMAL-p5X from New England Biolabs] can often produce a more soluble protein (Cat. No. E8200S) (Boon, Livingston, Chmiel, David, & Barton, 2003; Chmiel, Golinelli, Francis, & David, 2001; Liu, Xia, & Case, 2002; Vandevenne et al., 2013; Wiley, Murphy, et al., 2007). The pMAL Protein Fusion and Purification System contains a cloning site downstream of a *malE* gene encoding the 42.5 kDa MBP and results in expression of an MBP-fusion protein that increases protein solubility, while maintaining proper folding and biological activity (Kapust & Waugh, 1999). In some cases MBP appears to act as a chaperone to induce protein folding and stability (Kapust & Waugh, 1999). After expression, the MBP-fusion protein allows for simple purification using amylose affinity chromatography. The construction of the vector also places a linker containing 10 Asn residues between the MBP and protein of interest domains to inhibit significant binding interactions between the two proteins. As a result, the protein of interest is maintained in a more native environment away from the MBP tag and ensures the tag will be able to bind the amylose column efficiently during purification. The pMAL vector also incorporates a Factor Xa or Enterokinase recognition site immediately before the cloning region to allow cleavage of the MBP tag postpurification yielding native protein (Pavletich & Pabo, 1991). Furthermore, different pMAL vectors can allow protein expression in the cytoplasm or periplasm as desired by the user (Pattenden & Thomas, 2008). For added versatility, another cleavage site can be engineered into the expressed protein during cloning. For example, the recognition sequence of the tobacco etch virus (TEV) protease can be incorporated in the forward primer during

PCR (Kurz et al., 2006; Phan et al., 2002). Our laboratory uses the pMAL vector to clone ZFs with Fe–S clusters, as described here. We note that we have also produced CPSF30 with either a glutathione *s*-transferase or a hexahistidine tag. We find that the MBP tag produces the highest yields of soluble and active protein while also increasing our long-term storage stability.

2.1.1 Equipment

- Thermocycler
- Agarose gel running apparatus
- SPD1 SpeedVac Concentrator (Thermo Fisher)
- Light box
- Scalpel
- Centrifuge

2.1.2 Buffers and Reagents

- 10 × *Taq* DNA polymerase PCR buffer (200 m*M* Tris–HCl, 500 m*M* KCl, pH 8.4) (Thermo Fisher, Cat. No. 18067017)
- dNTPs
- $MgCl_2$
- Platinum Taq polymerase
- DH5α *E. coli* cells
- LB agar (10 g/L casein peptone, 5 g/L yeast extract, 5 g/L sodium chloride, and 15 g/L agar) (Affymetrix, Cat. No. 75851)
- Ampicillin (Sigma Aldrich, Cat. No. A9518)
- Ethidium bromide (Fisher, Cat. No. BP 1302-10)
- Tris/acetic acid/EDTA (TAE) buffer (Bio-Rad, Cat. No. 1610743)
- Qiagen miniprep kit (Qiagen, Cat. No. 27106)
- Qiagen PCR purification kit (Qiagen, Cat. No. 28104)
- Buffer 4 (NEB, Cat. No. B7004S)
- BSA (NEB, Cat. No. B9001S)
- *Nde*1 (NEB, Cat. No. R0111)
- *BamH*1 (NEB, Cat. No. R0136S)
- 6 × Loading dye (1 × contains 2.5% Ficoll-400, 11 m*M* EDTA, 3.3 m*M* Tris–HCl, 0.017% SDS, 0.015% bromophenol blue, pH 8.0) (NEB, Cat. No. B7021S)
- Qiagen gel extraction kit (Qiagen, Cat. No. 28704)
- Invitrogen Super Optimal broth with Catabolite repression (S.O.C.) media (2% tryptone, 0.5% yeast extract, 10 m*M* NaCl, 2.5 m*M* KCl, 10 m*M* $MgCl_2$, 10 m*M* $MgSO_4$, 20 m*M* glucose) (Thermo Fisher, Cat. No. 15544034)

2.1.3 Protocol

Note: As a general guide, the pMAL Protein Fusion and Purification System Instructional Manual (New England Biolabs) is followed with a few exceptions.

Primer design

1. Design primers, as an example CPSF30 primers are indicated:

   Forward: Noncoding (6 nucleotides)/restriction site (6 nucleotides)/TEV cleavage site (21 nucleotides)/CPSF30 DNA (24 nucleotides).

   5′-TTC TTC/CAT ATG/GAA AAT TTA TAT TTT CAA GGT/ATG GAC AAG TCA GGG GCT GCT GTC-3′

   Note: A start codon is not necessarily needed as the beginning of the MBP sequence contains a start codon.

   Reverse: Noncoding (6 nucleotides)/restriction site (6 nucleotides)/stop codons ×2 (6 nucleotides)/CPSF30 DNA (24 nucleotides).

   Note: DNA and stop codon sequences are reverse compliments of coding DNA.

   5′-TTC TTC/GGA TCC/TTA CTA/TTC AAA TCG AGG GTG CAT GAA TTT-3′

PCR setup

2. The following reagents are combined for the PCR experiment, and these values are adapted from recommendation by New England Biolabs (Biolabs, 2015).

Reagents	Volume (μL)	Final Concentration
Milli-Q water	34.5	—
PCR buffer (10 ×)	5	1 ×
$MgCl_2$	1.5	1.5 m*M*
dNTPs (10 m*M*)	1.5	3 m*M*
Forward primer (5 μ*M*)	3	0.3 μ*M*
Reverse primer (5 μ*M*)	3	0.3 μ*M*
Template DNA	1	—
Platinum Taq polymerase (5 μ/μL)	0.5	2.5 μ
Total volume	50	—

Note: Reagents are added to the PCR tube in the order listed.

PCR cycle

3. The PCR conditions explained here typically work well for ZF gene amplification in our lab. With other constructs, some steps (e.g., primer design, denaturation and annealing temperatures, length of extension times, etc.) may need to be varied to improve desirable yields.
   - **a.** Initial denaturation of template DNA at 94°C for 3 min
   - **b.** Denature double-stranded DNA at 94°C for 1 min
   - **c.** Anneal primers at 65°C for 1 min
   - **d.** Elongation of DNA at 72°C for 1 min
   - **e.** Repeat for 25 cycles
   - **f.** Final elongation step at 72°C for 15 min
   - **g.** Final hold at 4°C
4. Load the amplified PCR products onto a 1% agarose gel with ethidium bromide staining to ensure that the correct length of DNA was copied. The agarose gel should be prepared by adding 0.3 g of ultrapure agarose and 1 μL of ethidium bromide to 30 mL of 1 × TAE buffer and allowed to solidify in the gel apparatus.
5. Follow Qiagen's PCR purification kit and elute DNA using Milli-Q water and store the purified DNA at − 20°C (Qiagen protocol, Cat. No. 28104).
6. Load and run a 1% agarose gel, as previously described (step 4) with all PCR products and extracted pMAL-c5E plasmid to ensure the products and vector have been amplified successfully.

pMAL-c5E plasmid prep

The pMAL-c5E vector can be used as received, or amplified and stored as described here.

7. Transform 1 μL of pMAL-c5E plasmid into 50 μL of DH5α *E. coli* chemically competent cells by pipetting 1 μL of plasmid into a 50-μL aliquot of DH5α cells in a 1.8-mL Eppendorf tube and gently vortex the tube to mix the reagents.
8. Incubate on ice for 5 min.
9. Heat shock the plasmid and cell mixture for 45 s at 45°C.
10. Incubate on ice for 2 min.
11. Add 500 μL of S.O.C. media and triturate the solution to ensure proper mixing.
12. Incubate at 37°C for 45 min.
13. Plate 100 μL of the solution onto a LB agar plate containing 100 μg/mL ampicillin. Allow to incubate overnight at 37°C.
14. Remove the plates and allow them to cool to room temperature.

15. Select a single colony to grow in an overnight flask of 50 mL containing 100 μg/mL of ampicillin at 37°C.
16. The 50 mL overnight cultures of pMAL-c5E vector should be centrifuged at 5250 × *g* at 4°C for 10 min.
17. Isolate the DNA via a Qiagen miniprep kit (Plasmid Miniprep Kit: QIAprep Spin Miniprep Kit-Cat. No. 27106).
18. Elute the DNA with Milli-Q water and store at −20°C.

Double digest using Nde*1 and* BamH*1*

19. Dry all samples for 1 h in vacuo in a SpeedVac concentrator.
20. Using New England Biolabs "double digest finder," find compatible working conditions for both digestion enzymes. For *Nde*1 and *BamH*1, Buffer 4 was used with BSA at 37°C for 2 h.
21. Resuspend the pMAL-c5E vector in 32 μL of Milli-Q water and PCR product in 15.8 μL so that each is at a concentration of about 25 ng/μL.
22. Add the following to each reaction.
    a. 2 μL of Buffer 4
    b. 0.5 μL of BSA
    c. 1 μL of *Nde*1
    d. 1 μL of *BamH*1
23. Incubate for 2 h at 37°C.

    Note: If the double-digestion step does not produce satisfactory yields of digested DNA, single digests of the plasmid with each restriction enzyme should be performed followed by analysis on a 1% agarose gel to verify that both restriction enzymes are active.
24. Add 2 μL of 6 × loading dye to each reaction mixture and load 10 μL per well on a 1% agarose gel. Run the gel at room temperature for 50 min, or until the loading dye is approximately 80% down the gel, at 100 V.

    Note: Voltage can typically be varied between 80 and 150 V depending on the concentration of agarose in the gel to prevent it from overheating.
25. Excise the bands from the gel using a light box and scalpel.
26. Follow Qiagen's gel extraction kit and elute DNA using 50 μL of Milli-Q water (Plasmid Miniprep Kit: QIAprep Spin Miniprep Kit-Cat. No. 28704)
27. Remove 1 μL aliquot of each reaction to verify purity by 1% agarose gel as previously described.
28. Dry samples in SpeedVac for 35 min.

Ligation

29. We find that ligation is best performed by testing several ratios of plasmid to insert and then selecting the best product for future studies.

	Reaction A (μL)	Reaction B (μL)	Reaction C (μL)	Reaction D (μL)
Ligase	1	1	1	1
10× Ligase buffer	2	2	2	2
Insert DNA	1	3	4	5
Plasmid DNA	7	5	4	3
Water	9	9	9	9
Total volume	20	20	20	20

30. Incubate the ligation reactions for 10 min at room temperature and then transform as previously described (step 7) into DH5α *E. coli* cells with the following exception: 5 μL of ligation mixture into 50 μL of cells.
31. Plate 150 μL of transformed cells onto LB agar plates containing 100 μg/mL of ampicillin.
32. Incubate the LB agar plates overnight at 37°C.
33. Choose a single colony from the plate and grow overnight in 50 mL of sterilized LB containing 100 μg/mL of ampicillin at 37°C with shaking at 230 rpm.
34. Spin down overnight culture in a 50-mL conical tube at 5250 × *g* for 10 min at 4°C.
35. Follow the Qiagen mini prep kit (Cat. No. 27106) to extract the DNA; use 50 μL of Milli-Q water to elute the DNA.
36. Store at −20°C.
37. Aliquot 10 μL of each sample to verify ligation by 1% agarose gel.
38. Dilute sample with 5.8 μL of Milli-Q water and perform a single digestion of the ligated product using one of the restriction enzymes chosen during ligation.
39. Add 2 μL of DNA 6× loading buffer and run a 1% agarose gel as previously described.

Note: A successful ligation should result in the presence of a single band on the agarose gel at the length of the pMAL-c5E plasmid plus the length of your gene of interest. If only the plasmid (no insert) is observed, a different colony should be selected.

40. Quantitate DNA concentration by ultraviolet–visible spectroscopy (UV–vis) at A_{260}. Dilute 3 μL of pure DNA in a cuvette containing 500 μL of Milli-Q water and run full spectrum analysis.

    Concentration can be determined by:

$$[\text{DNA}] = (50\mu g/\text{mL}) \times (\text{dilution factor}) \times A_{260}$$

    Example

$$[\text{DNA}] = (50\mu g/\text{mL}) \times (503\mu L/3\mu L) \times (0.023924)$$
$$[\text{DNA}] = 200\,\text{ng}/\mu L$$

    Note: 50 μg/mL is used to quantify dsDNA. For ssDNA and RNA 33 μg/mL and 40 μg/mL can be used, respectively (Barbas, Burton, Scott, & Silverman, 2007).
41. The purity of the sample can be determined by a ratio of A_{260}/A_{280}. The sample should have a ratio of 1.7–2.0 as pure DNA is ~1.8 (Barbas et al., 2007).
42. Concentrate the sample in vacuo to the concentration desired by the sequencing group you are using. For example, we needed samples at approximately 300 ng/μL.
43. Submit samples for DNA sequencing and verify that the correct sequence has been inserted and that the MBP and insert are in the correct reading frame.

3. EXPRESSION OF ZF PROTEINS AND ADAPTATIONS FOR INCLUSION OF IRON–SULFUR CLUSTERS

After the protein of interest has been successfully incorporated into your chosen vector, it needs to be overexpressed, retrieved from within the cell, and maintained in a soluble aqueous fraction. In this section, we describe our expression protocols as well as how to utilize sonication to obtain a desired protein from a cell pellet postinduction. As a reference, we have included sample data from CPSF30 in Fig. 3.

3.1 General Protocol for Expression of Zinc Finger Proteins Containing Iron–Sulfur Clusters

Optimizing bacterial growth mediums and expression conditions play an essential role in successful protein overproduction. We express zinc finger proteins using BL21 (DE3) *E. coli* cells in Lennox Luria Bertani Broth (LB) BL21 (DE3) cells (Invitrogen/Thermo Fisher, Cat. No. C600003). LB is

one of the most commonly used growth mediums for cultivating *E. coli* since it was first described by Bertani (1951) and Larentis et al. (2014). BL21 (DE3) cells have high transformation efficiency, express T7 polymerase during isopropyl β-D-1-thiogalactopyranoside (IPTG) induction, and are deficient of Lon and OmpT proteases making it suitable for overproduction of nontoxic proteins (Newton, Mackay, & Crossley, 2001; Rosano & Ceccarelli, 2014).

Once the bacterial strain and growth medium have been selected, the growth conditions need to be optimized. Varying induction temperature, IPTG concentrations, shaking speed, and media supplementations can have large effects on protein yield and quality (Larentis et al., 2014). By reducing the induction temperature or IPTG concentration, bacterial growth and protein expression can be slowed down (Larentis et al., 2014). This can be beneficial if the protein of interest is being expressed too quickly and yielding low-quality or misfolded protein (Larentis et al., 2014). We typically overexpress zinc finger proteins at 37°C with a final IPTG concentration of 1 m*M*; however, if expression levels are not satisfactory, we alter the temperature and/or IPTG concentration. Incubator shaking speeds affect culture aeration, and higher speeds can help accommodate higher cell densities in the culture and increase protein yields (Larentis et al., 2014). To maintain proper aeration, we utilize a production volume of 1 L in 4-L Erlenmeyer flasks and a shaker speed of 230 rpm. Some laboratories have shown success expressing zinc finger proteins in BL21 cells without the need of supplementing their media (e.g., metals, metal donors, scaffold donors, etc.) as seen with GATA-1 and MBNL (Newton et al., 2001; Warf & Berglund, 2007), while other labs have shown that additional supplementation to the growth media during induction is needed to increase protein quality and biological activity. This has been observed with HIV-1 NC and a zinc finger protein designed by Sangamo Biosciences (Lee, De Guzman, Turner, Tjandra, & Summers, 1998; Liu et al., 2002). For expression of ZF proteins in our laboratory, we supplement the media with $ZnCl_2$ to improve zinc incorporation yields and 0.2% glucose to ensure it is the primary carbon source. For supplementation of iron to aid Fe–S cluster assembly we have recently begun to supplement with $FeCl_3$; for a more in-depth study of supplementation and Fe–S cluster incorporation yields, we refer you to the work of Jaganaman, Pinto, Tarasev, and Ballou (2007). This helps facilitate increased incorporation of the zinc and Fe–S clusters into the protein thereby improving overall activity. Another approach to optimize Fe–S cluster loading is to utilize a minimal media/metal supplementation approach which provides the essential salts and sugars that are required for cell growth. Booker and Krebs describe this protocol for the expression of RlmN and AstB Radical SAM proteins

(Lanz et al., 2012). This allows the levels of metal ions that are present in the growth media to be controlled, in contrast to LB broth, which contains variable levels of metal ions (including iron and zinc). Our general expression protocol for CPSF30 is described later.

3.1.1 Equipment

- Incubating Orbital Shaker, Model 3500I (VWR, Cat. No. 12620-946)
- Innova Orbital Shaker
- 250-mL Erlenmeyer flasks
- 4-L Erlenmeyer flasks
- Avanti J-20 XPI centrifuge (Beckman Coulter, SKU# 8043-30-1171)
- J-LITE® JLA-10.500 Rotor Assembly with 500-mL bottles and aluminum canisters (Beckman Coulter, Cat. No. 369681)
- Table top microcentrifuge equipped for 1.5-mL Eppendorf tubes (Denville Scientific, Cat. No. C0260-24)
- Lambda 25 UV–vis Spectrometer (Perkin Elmer, Cat. No. L600000B)
- Autoclave
- Mini-PROTEAN® Tetra Vertical Electrophoresis Cell (Bio-Rad, Cat. No. 1658004)
- Oscillating platform shaker (Stovall Life Sciences, Cat. No. BDRAA115S)
- Fisher Scientific dry bath incubator (Boekel, Cat. No. 110011)

3.1.2 Buffers and Reagents for LB Overexpression

- Milli-Q water system
- Invitrogen S.O.C. media (Thermo Fisher, Cat. No. 15544034)
- Lennox LB broth (American Bioanalytical Inc., Cat. No. AB01198)
- 100 mg/mL ampicillin prepared from ampicillin sodium salt (Sigma Aldrich, Cat. No. A9518)
- LB broth containing 0.2% glucose
- 100 m*M* $ZnCl_2$ (Sigma Aldrich, Cat. No. Z0152)
- 1 *M* IPTG (Research Products International Corp through Fisher Scientific, Cat. No. 50-488-727)
- 2 × Laemmli Sample Buffer (Bio-Rad, Cat. No. 1610737)
- 1 × SDS-PAGE running buffer (25 m*M* Tris base, 19 m*M* glycine, and 3.5 m*M* SDS)
- Invitrogen BenchMark Protein Ladder (Thermo Fisher, Cat. No. 10747012)
- Coomassie blue stain (3 m*M* Coomassie blue in 50% methanol, 10% acetic acid, and 40% Milli-Q water by volume)
- Destain (25% methanol, 10% acetic acid, and 65% Milli-Q water by volume)

3.1.3 Protocol

Day 1

1. Prepare overnight culture medium by adding 1 g of LB media to 50 mL of Milli-Q water.

   Note: We typically set up these cultures in duplicate in case one of the overnight cultures fails to grow.
2. Cover flasks with tin foil and autoclave the media for 20 min at 250°C.
3. Pipette 2 μL of the plasmid into a 50-μL aliquot of BL21 (DE3) cells in a 1.5-mL Eppendorf tube and flick the bottom of the tube to mix.
4. Incubate on ice for 5 min.
5. Heat shock the plasmid and cell mixture for 45 s at 45°C.
6. Incubate on ice for 2 min.
7. Add 500 μL of S.O.C. media and triturate the solution to ensure proper mixing.
8. Incubate at 37°C for 45 min.
9. Remove the overnight media from autoclave and allow to cool to room temperature (~30 min).
10. Pipette 50 μL of 100 mg/mL ampicillin into the overnight flasks and swirl gently to mix achieving an effective concentration of 100 μg/mL.
11. Pipette 150 μL of transformed cells into the overnight flasks.

    Note: LB agar plates containing 100 μg/mL of ampicillin could be made as well to save colonies for future overnight flasks.
12. Incubate the transformed cells in an incubating orbital shaker at 37°C with shaking at 230 rpm overnight for 12–16 h.
13. Prepare 1 L of induction media containing 0.2% glucose by adding 20 g of LB and 2 g of glucose to 1 L of Milli-Q water.
14. Cover flasks with tin foil and autoclave for 20 min.
15. Allow induction media to cool to room temperature.

    Note: Induction media can be left at room temperature overnight if tin foil is not removed and handled aseptically after autoclaving.

Day 2

1. Inoculate 1 L induction media with 15 mL of overnight culture.
2. Incubate induction flask at 37°C with shaking at 230 rpm.
3. Acquire 1 mL aliquot and obtain a starting UV–visible measurement at 600 nm.
4. Monitor protein induction over time by taking 1 mL aliquots and measuring the absorbance at 600 nm.

5. When the flask reaches an absorbance at 600 nm of approximately 0.3, supplement the media with 1 mL of 100 m*M* $ZnCl_2$ to reach an effective concentration of 1 m*M* Zn.
6. When the flask reaches an absorbance of 0.5–0.6 at 600 nm take 1 mL aliquot to reserve for SDS-PAGE analysis and induce with 1 mL of 1 *M* IPTG achieving an effective concentration of 0.1 m*M*.
7. Collect and preserve 1 mL aliquots of cells every hour to be used for SDS-PAGE analysis.
8. At 3 h postinduction stop the protein expression and centrifuge induction media at 7800 × *g* for 20 min at 4°C.

   Note: It is recommended to perform inductions in batches of two or four to allow simple balancing of the centrifuge. If only one batch is prepared, the centrifuge can be balanced using a bottle containing only water of identical weight.
9. Remove supernatant and store cell pellets at −20°C.

SDS-PAGE analysis

An example of SDS-PAGE analysis of CPSF30 is shown in Fig. 3B.

1. Pellet 1 mL aliquots by microcentrifugation and remove supernatant.
2. Resuspend cell pellets in 100 μL of Milli-Q water and add an equal volume of 2 × Laemmli sample buffer.
3. Incubate resuspended cell pellets on a heat block at 90°C for 3–5 min.
4. Run 5–15 μL of each sample on a 15% SDS-PAGE until the ladder reaches about 2 cm from the bottom of the gel.
5. Carefully remove the gel from the glass plates and transfer it to a suitable container for staining.
6. Add enough Coomassie blue stain to cover the gel and agitate for 30–60 min using an oscillating rocker.
7. Remove Coomassie blue stain and add enough destaining solution to cover the gel and return to the oscillating rocker.

   Note: Destaining solution may need to be exchanged with fresh solution two or three times.
8. Destain until background Coomassie stain dissipates and the protein bands can be resolved.
9. Wash remaining destaining solution from the container and the gel can be stored in Milli-Q water.

   Note: It is advised that the gel be imaged immediately for record keeping. Although the gel can be stored for up to 1 week in water, microbial growth and gel swelling can begin to obfuscate the bands. Be careful not to allow the water to evaporate, as the gel will dry, shrink,

and become brittle. For storage of up to several weeks, gels can be stored in 5% acetic acid at 2–8°C. If the gel is being retained for further analysis or for a laboratory notebook it can be stored dry as previously described or through commercially available gel drying instruments (Smith, 1994).

3.2 Cell Lysis

Once CPSF30 has been successfully overexpressed as evidenced by an enhanced band on SDS-PAGE, the protein must be extracted and purified from the expression cells. Unless your protein has been engineered to be excreted from the cell during expression, the plasma membrane must be ruptured to release the protein of interest. There are many different techniques available to disrupt the cell membrane and extract the protein of interest. These include sonication, freeze–thaw, enzymatic digestion, chemical digestion, and French press. Our laboratory finds that sonication is an effective strategy to lyse cells containing overexpressed ZFs. Sonication uses ultrasonic sound waves to produce liquid shear and cavitation that subsequently disintegrates the cell wall of the bacteria. Cavitation is the formation, growth, and collapse of vapor bubbles created by high intensity sound waves (Feliu, Cubarsi, & Villaverde, 1998; Ho et al., 2006). The collapse of these vapor filled bubbles causes intense local shock up at levels of thousands of atmospheres disrupting the cells around them (Ho et al., 2006). One of the main drawbacks of sonication is the heat generated (Feliu et al., 1998). To overcome the potential risk of denaturing the protein at high heat, it is advised that the samples are kept on ice and sonication methods be optimized to short durations of pulses with resting periods to allow the sample to cool (Feliu et al., 1998).

3.2.1 Equipment

- Fisher Scientific Sonic Dismembrator Model 100 (Fisher, Model No. XL2000-350R)
- Avanti J-20 XPI centrifuge (Beckman Coulter, SKU# 8043-30-1171)
- JA-25.50 Fixed-Angle Rotor equipped with 50-mL centrifuge tubes (Beckman Coulter, Cat. No. 363055)

3.2.2 Buffers and Reagents

- Lysis buffer (20 m*M* Tris, 200 m*M* NaCl, adjust pH to 7.5 using NaOH or HCl)
- Pierce™ Protease Inhibitor Tablets, EDTA free (Thermo Scientific, Cat. No. 88266)

3.2.3 General Sonication Protocol

1. Remove the cell pellet from −20°C storage and place on ice.
2. Add one protease inhibitor tablet and resuspend the pellet in 25 mL of lysis buffer.
3. Split the resuspended pellet into two equal fractions in 50-mL centrifuge tubes.
4. Sonicate one fraction at 22.5 kHz on level 6 of 10 for 20 s on ice.

   Note: Sonicator tip should be submerged approximately half way into the solution and gently moved around without touching the walls of the centrifuge tube.
5. Let the solution rest on ice for 40 s.
6. Repeat steps 4 and 5.
7. Sonicate the fraction at 22.5 kHz on level 7 of 10 for 20 s.
8. Let the solution rest on ice for 40 s.
9. Repeat steps 7 and 8.
10. Repeat steps 4–9 with the other fraction.
11. Centrifuge both fractions for 20 min at 12,100 rpm (20,000 × *g*) at 4°C.
12. Combine both supernatants to form the load for amylose column purification.

    Note: Retain aliquots of both the pellet and lysate for SDS-PAGE analysis.

If you have an Fe–S cluster present, the supernatant will remain reddish-brown (Fig. 3C).

4. PROTEIN PURIFICATION

After conditions have been optimized to keep the protein of interest stable and soluble after expression, the protein must be isolated from the rest of the host cell's proteins. In this section, we discuss how to purify CPSF30 using amylose column chromatography and a polishing step using size exclusion chromatography. As a guide, we have included sample data from CPSF30 in Fig. 4.

4.1 Amylose Column Chromatography

CPSF30 includes an MBP tag, which allows us to utilize amylose chromatography to purify. This approach works well for all MBP ZFs our laboratory has investigated. In the cell, MBP mediates various maltodextrin metabolism pathways recognizing any alpha-(1 → 4)-D-glucose polysaccharide over eight repeating units (Pattenden & Thomas, 2008). Amylose

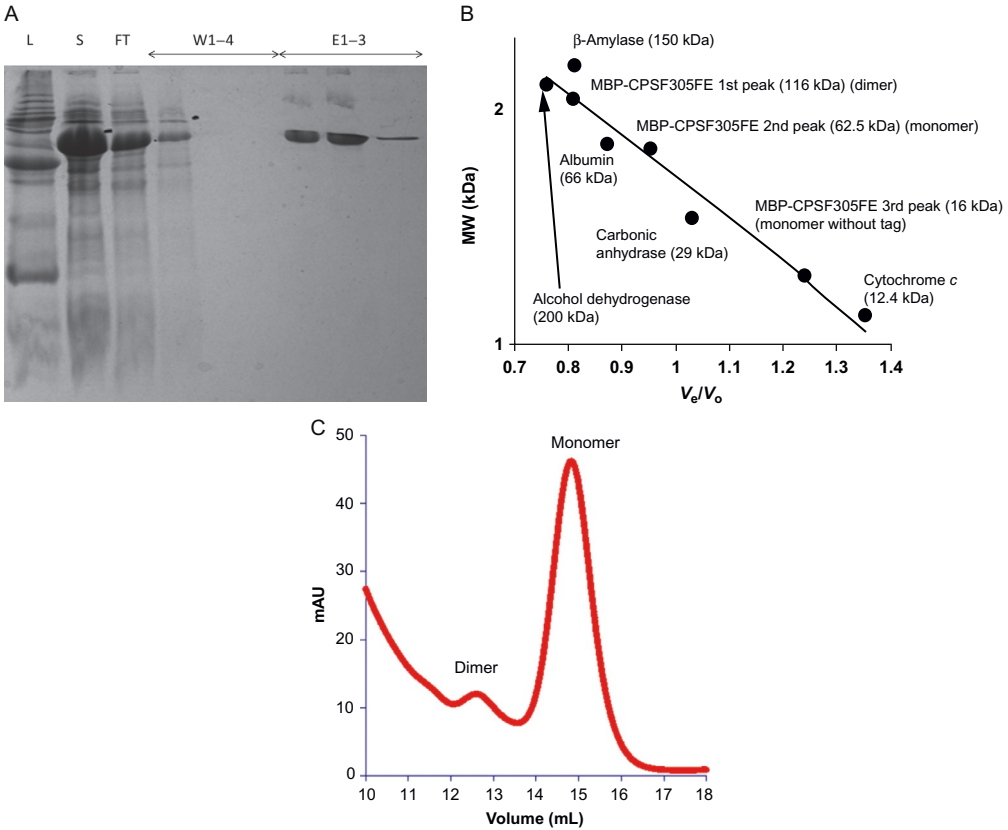

Fig. 4 The purification steps for CPSF30. (A) 15% SDS-PAGE of CPSF30 postamylose column chromatography. *E1–3* = elution 1–3, *FT* = flow-through, *L* = Invitrogen BenchMark Protein Ladder (Thermo Fisher), *S* = supernatant, *W1–4* = wash 1–4. (B) Calibration curve utilizing Sigma Aldrich gel filtration markers kit for protein molecular weights 12,000–200,000 Da used to determine the molecular weight of MBP-CPSF30. (C) UV–visible monitored chromatogram of MBP-CPSF30 during purification via Superdex 10/300. Both the dimer and monomer forms are shown.

affinity column chromatography takes advantage of this native-binding interaction by incorporating repeating maltose polymers with these alpha-(1 → 4) linkages covalently bonded to agarose beads in a stationary phase to work in a bind and elute purification procedure. This makes for a specific and effective purification method that can yield pure protein after just one purification step and we often obtain >95% purity of ZFs of interest. MBP's high activity in diverse environments increases its appeal as a purification method as it allows for a wide range of buffer conditions varying pH and ionic strength without sacrificing purification yields. The most common buffer conditions with high yields still remain around neutral pH at about 7.5–8.0 and salt concentrations in the range of 100–500 m*M* (Pattenden & Thomas, 2008). At high enough protein concentrations, MBP can affect pH as it has an acidic isoelectric point so higher buffering capacity is ideal, and it is generally recommended to have concentrations of at least 20 m*M* (Pattenden & Thomas, 2008). Even though purification of MBP using amylose column chromatography is highly robust, it does have some caveats. Nonionic detergents like Triton X-100, polysorbate 20, and other additives that inhibit hydrophobic interactions should be avoided during the purification process as they can reduce column loading capacity and result in lower purification yields (Pattenden & Thomas, 2008). Additionally, carbon sources in the induction media other than glucose should be avoided as they can upregulate expression of maltose scavenging proteins when maltodextrin concentrations are depleted. These scavenging proteins can make their way into the sonicated lysate and can bind, modify, or release maltose from the stationary phase of the column-decreasing loading capacity and allowing MBP loss in the flow-through (Pattenden & Thomas, 2008). To ensure glucose is the primary carbon source in our media, we supplement with an additional 0.2% glucose when expressing CPSF30 (Shimberg et al., 2016).

4.1.1 Equipment

- Glass Econo-Column® Columns 2.5 cm × 20 cm (Bio-Rad, Cat. No. 7374252)
- 50-mL conical tubes
- 3.5 kDa Dialysis tubing (VWR, Cat. No. 28170-166)
- Amicon Ultra-15 Centrifugal Filter Unit with Ultracel-30 membrane (Millipore, Cat. No. UFC903008)
- SDS-PAGE instrumentation as previously described

4.1.2 Buffers and Reagents

- Wash buffer (20 m*M* Tris, 200 m*M* NaCl, pH adjusted to 7.5)
- Elution buffer (20 m*M* Tris, 200 m*M* NaCl, 10 m*M* maltose, pH adjusted to 7.5)
- Amylose resin (New England Biolabs, Cat. No. E8021S)

  Note: The amylose resin has a binding capacity of 6–8 mg/mL of protein to column bed volume. 15 mL of amylose resin can be used for up to 100 mg of crude MBP-fusion protein at a time
- Dialysis buffer (20 m*M* Tris, 50 m*M* NaCl, pH adjusted to 7.0)
- Storage buffer (20% ethanol)
- SDS-PAGE buffers and reagents as previously described

  Note: Wash, elution, and dialysis buffers can vary depending on the protein of interest's stability in various pH, ionic strength, and buffering capacity conditions. These properties are usually determined empirically.

4.1.3 General Amylose Affinity Column Chromatography Purification Protocol

Note: Our purification procedure is performed at room temperature, but if protein stability is a concern, all steps may be performed in a cold room at 4°C.

1. Slurry the resin in 20% ethanol and add to column.
2. Allow the resin to form a gravity settled bed at the bottom of the column.
3. Equilibrate the column flowing through excess wash buffer (at least five column volumes).
4. Load cell lysis supernatant onto amylose column and seal the column.
5. Place the loaded column on an orbital rocker and rock for 15–20 min.
6. Allow the resin to form a gravity packed bed and open the bottom valve of the column capturing the flow-through until the supernatant is just above the resin bed.

   Note: Be careful to never let the column run dry at any time during the purification process.
7. Add 45 mL (three CVs) of wash buffer to the column and capture it in a new 50-mL conical tube. Place captured fractions on ice until purification procedure is completed.
8. Repeat step 7 three more times capturing each wash in a new conical tube.
9. Add 15 mL (one CV) of elution buffer and capture the flow-through.
10. Repeat step 9 two more times.
11. Retain 50 μL aliquots of all fractions for SDS-PAGE analysis.

12. Once purification has been verified by SDS-PAGE, combine all elution fractions containing pure protein and pipette protein solution into dialysis tubes for buffer exchange.

    Note: Dialysis tubing should be incubated in dialysis buffer for at least 5 min before filling with protein solution.
13. Place tubing containing protein in 4 L of dialysis buffer to exchange overnight at 2–8°C.
14. Concentrate protein samples to approximately 100–250 μ*M* using Amicon spin filters by centrifuging at 4000 × *g* for 25 min at 4°C.
15. Repeat concentration (step 14) by removing filtrate and adding elution fractions until all fractions are concentrated to approximately 1.5–5.0 mL.
16. Fill retentate side of spin filter with fresh dialysis buffer and centrifuge at 4000 × *g* for 25 min at 4°C.
17. Repeat step 16 two more times.
18. If pure, aliquot samples for storage at −80°C or store/prepare samples for size exclusion chromatography.
19. Add storage buffer to column and allow approximately three column volumes to flow-through. Store column in excess storage buffer at 4°C. The column can be regenerated by washing as follows: Milli-Q water (three CVs), 0.1% SDS (three CVs), Milli-Q water (one CV), and wash buffer (five CVs). The column is then ready to be loaded again.

    Note: Amylose resin can be reused up to five times.

A typical SDS-PAGE of purified CPSF30 (>95% purity) is shown in Fig. 4A.

4.2 Additional Polishing Step via Size Exclusion Chromatography

CPSF30 is typically obtained at >95% purity after one amylose column. If desired, CPSF30 can be further purified using size exclusion chromatography (also known as gel filtration chromatography). This method separates impurities based upon size. A standard curve for molecular weights should be constructed using a gel filtration markers kit for protein molecular weights 12,000–200,000 Da (Sigma Aldrich) on a Superdex 200 10/300 gel filtration column (GE) (Gel Filtration Molecular Weight Markers Kit for Molecular Weights 12,000–200,000 Da Technical Bulletin, n.d.). This kit uses six standard proteins to construct a calibration curve that can be used to determine molecular weights of proteins in a mixed sample. These standards are cytochrome *c* (12.4 kDa), carbonic anhydrase (29 kDa), bovine serum albumin (66 kDa), alcohol dehydrogenase (150 kDa), β-amylase

(200 kDa), and blue dextran (2000 kDa). Blue dextran is not used in the calibration curve, but is used to determine the void volume of the column as it does not interact with the bead's pores and elutes at the solvent front (Gel Filtration Molecular Weight Markers Kit for Molecular Weights 12,000–200,000 Da Technical Bulletin, n.d.). This allows normalization of the elution volume measurements of the other five calibration standards. The ratio of elution volume (V_e) to void volume (V_o) (V_e/V_o) can be determined for each standard allowing the calibration curve to estimate the molecular weight of unknown proteins (such as MBP-CPSF30 vs contaminants) (Gel Filtration Molecular Weight Markers Kit for Molecular Weights 12,000–200,000 Da Technical Bulletin). The calibration needs to be performed each time the size exclusion column is used as retention rates can shift slightly when the column is moved from one location to another changing packing factors or internal bead densities. Fig. 4B gives an example of CPSF30 that has been purified via size exclusion chromatography and referenced to the calibration curve. Prior to loading the column, it is important to centrifuge your sample on a table top centrifuge (Denville) at 14,000 rpm for 10–15 min to remove any aggregates in the protein sample that could damage the FPLC system or the column. The sample can then be loaded onto the Superdex 200 10/300 column (we use an AKTA Pure FPLC (GE) with Unicorn software) (AKTA pure: User Manual, 2012). The flow rate should be experimentally optimized to ensure proper separation of your protein of interest from other impurities; we use a flow rate of 0.4 mL/min (31 cm/h) to purify CPSF30. Fig. 4C shows the chromatogram for purification of CPSF30.

5. METHODS TO CHARACTERIZE ZF PROTEINS WITH Fe–S CLUSTERS

To characterize ZF proteins isolated with an Fe–S cluster, three methods are typically employed: optical spectroscopy to visualize thiolate-to-Fe(III) charge-transfer, ICP-MS (inductively coupled plasma mass spectrometry) to quantify iron and zinc, and XAS (X-ray absorption spectroscopy) spectroscopy to determine metal oxidation states, geometry at the metal center, and ligand identity. We perform spectroscopy and ICP-MS at Maryland, and our protocols are described later. XAS spectroscopy is performed by our collaborator, Tim Stemmler (Wayne State University), and we refer you to our published collaborative work (Shimberg et al., 2016).

5.1 Protein Characterization Using UV–vis

UV–visible spectroscopy can be utilized to determine the concentration, purity, and presence of any iron–sulfur cofactors in newly identified "zinc finger" proteins (Adrover, Howes, Iannuzzi, Smulevich, & Pastore, 2015; Mapolelo, Zhang, Naik, Huynh, & Johnson, 2012; Miller, McLachlan, & Klug, 1985). In a typical experiment, an optical spectrum from 200 to 800 nm is obtained. Absorbance peaks at 220 and 280 nm, which correspond to backbone amide residues and aromatic side chains (tyrosine, tryptophan, and phenylalanine) respectively are then identified. The protein concentration can be determined utilizing Beer's law, $A_{280} = \varepsilon bc$, where A is the absorbance of the sample in absorbance units, ε is the molar absorptivity in L mol^{-1} cm^{-1} (often measured at 280 nm), b is the path length of the sample in cm, and c is the concentration of the sample in mol L^{-1}. In some cases, zinc finger protein copurify with nucleic acids, and these are often detected by the presence of an additional absorbance peak at 260 nm from purine and pyrimidine residues (Miller et al., 1985). The presence of an iron–sulfur cluster in a "zinc finger" can also be detected via UV–visible spectroscopy as charge transfer bands between 220 and 600 nm (Adrover et al., 2015; Dailey, Finnegan, & Johnson, 1994; Mapolelo et al., 2012). Fig. 5 shows the UV–visible spectra of CPSF30 loaded with both zinc and the Fe–S site as well as the Fe–S only species. Absorbance bands at 340, 420, 456, and 583 nm are observed for CPF30.

5.1.1 Equipment

- UV–vis
- Quartz cuvette

5.1.2 Buffers and Reagents

- 20 m*M* Tris, pH 7.0, 50 m*M* NaCl

5.1.3 General UV–vis Characterization Protocol for Proteins Containing Zinc Finger and Iron–Sulfur Clusters

Note: Our method is performed under aerobic conditions, but if iron oxidation is a concern, UV–vis characterization should be done in the absence of an oxygen atmosphere as previously described (Adrover et al., 2015; Mapolelo et al., 2012).

1. Add approximately 500 μL of dialysis buffer to the cuvette and insert into spectrophotometer

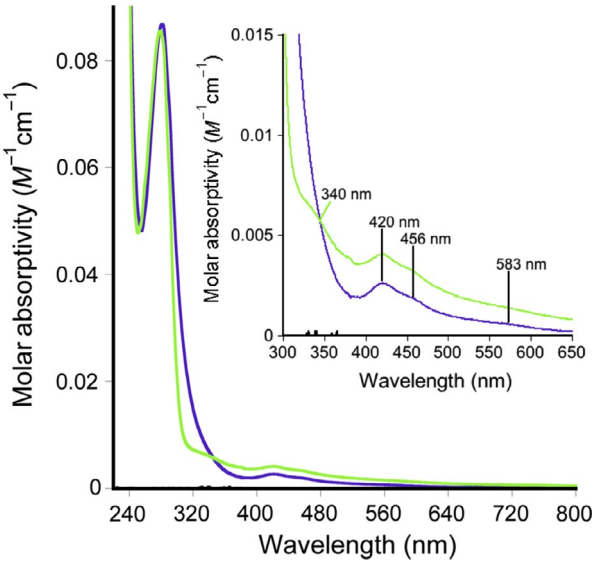

Fig. 5 Full UV–visible spectrum of CPSF30 protein in 20 m*M* Tris, 100 m*M* NaCl, pH 8, after purification. (*Inset*) Close up of 300–650 nm range denoting the Fe–S cluster charge transfer peaks. The *green band* shows the spectrum of isolated CPSF30 with both Fe and Zn bound; the *blue band* is the spectrum observed upon Zn chelation (Fe-only spectrum).

2. Blank the cuvette
3. Add 150 μL of pure protein solution and mix
4. Run a full UV–vis scan between 200 and 800 nm
5. Analyze spectrum for peaks around 280, 260, and between 300 and 600 nm.

   Note: If spectrum reaches maximum absorbance, a dilution may be necessary and the experiment will have to be repeated.
6. Calculate protein concentration using Beer's law ($A = \varepsilon bc$) and solve for concentration

   Note: If ε has not been determined empirically for your protein, a theoretical estimate can be obtained from http://web.expasy.org/protparam/. This estimate can vary slightly from actual molar absorptivity values in solution as protein folding, pH, and ionic strength can affect some aromatic residue's ability to absorb light (Simonian & Smith, 2006).
7. Look for peaks indicative of the presence of a $[2Fe—2S]^{2+}$ cluster or $[4Fe—4S]^{2+}$ cluster between 300 and 600 nm.

5.2 ICP-MS

ICP-MS is utilized to determine the metal content of proteins. ICP-MS is extremely sensitive—concentrations as low as one part per quadrillion can be theoretically measured (ppq) (Profrock & Prange, 2012). The instrument ionizes the sample with inductively coupled plasma and then the ionized sample is passed through a mass spectrometer to separate and quantify the metal/nonmetal ions (Zoorob, McKiernan, & Caruso, 1998). ICP-MS works with better speed, precision, and sensitivity to determine metal ions compared to inductively coupled plasma atomic emission spectroscopy (ICP-AES) which can also be used to determine metal content of proteins (Rommers & Boumans, 1996). The plasma used for ICP-MS is energized by heating argon gas with an electromagnetic coil, which generates electrically conductive argon ions that can interact with an aerosol sample to ionize elements for detection. The sample is converted into an aerosol by passing through a nebulizer to create consistent droplet sizes to interact with the charged argon gas. This is important to remove any large droplets from the sample and increase reproducibility of detection. An accurate calibration curve is integral to the instrument's ability to quantify the analytes of interest and should be conducted for each batch of samples. It is also important to utilize internal standards within the samples to monitor matrix effects. Matrix effects occur when a component of the sample, other than the analyte of interest, skews the reported values of detection, and enhance or suppresses the signal. Matrix effects can be monitored by quantifying a known element in a neat sample vs the same element spiked concentration in your matrix. Another caveat to ICP-MS when working with ^{56}Fe determination is interferences by $^{40}Ar^{16}O^{+}$ and $^{40}Ca^{16}O^{+}$ which have a molecular weight of 56 like iron and similar ionization states (Segura, Madrid, & Cámara, 2003). One way to overcome this interference is to use a helium (He) collision chamber before the detector. The He collision mode differentiates monoatomic elements vs polyatomic species by kinetic energy discrimination (McCurdy, Woods, & Potter, 2006). Since diatomic species have a larger cross-sectional area, they are prone to more collisions and move slower through the collision cell. This allows the monoatomic elements (^{56}Fe) with the same mass to pass to the detector with less interference and allows analysis down to concentrations as low as parts per billion (ppb). We routinely use a helium collision chamber for our analysis. Secondarily, ^{57}Fe can be analyzed with lower interference, but due to its lower abundance, sensitivity can be an issue.

ICP-MS protocol

1. Prepare 1 μ*M* CPSF30 in 5 mL 2% trace metal nitric acid (Fisher). 150 μL internal standard (100 μg/mL Bi, Ge, In, Li, Lu, Rh, Sc, and Tb; Agilent Technologies) is added to samples to ensure accuracy.
2. Zinc and iron calibration standards ranging from 0 to 500 ppb Zn/Fe are created using iron and zinc atomic absorption standard dilutions (Fluka Analytical).
3. Zinc and iron levels are detected on an Agilent 7700 × ICP-MS using an octopole reaction system in HE mode, an rf power of 1550 W, an argon carrier gas flow of 1.0 L/min, argon make-up gas flow of 0.1 L/min, helium gas flow of 4.5 mL/min, octopole rf of 160 V, QP bias of −15 V, and OctP bias of −18 V.
4. Data analysis was performed using the Agilent 7700 × ICP-MS instrument provided Mass Hunter software.

   Note: In a molar ratio, we usually see 0.5–1.7 equivalents of iron and 3.1–3.7 equivalents of zinc to CPSF30.

5.3 XAS Sample Preparation

To determine the geometry at the metal site, the ligands involved in coordination and metal oxidation state of ZF/Fe–S hybrid proteins, XAS is a common approach (Shimberg et al., 2016). Below we describe our protocol for sample preparation.

Protocol

1. CPSF30 samples are prepared in 20 m*M* Tris, 50 m*M* NaCl, pH 7 with 30% glycerol. Metal concentrations of CPSF30 are confirmed via ICP-MS analysis with metal concentrations greater than 0.5 m*M* of either Zn or Fe.
2. Samples are loaded into lucite XAS cells, prewrapped with kapton tape, flash-frozen in liquid nitrogen, and stored in liquid nitrogen until data collection.

6. ACTIVITY ASSAYS TO ASSESS DNA OR RNA BINDING FOR ZF/Fe–S HYBRID PROTEINS

Once isolated, the function of a ZF/Fe–S hybrid protein must be assessed. ZFs typically bind to other macromolecules (e.g., DNA or RNA) to promote transcription or translation (Brown, 2005). In addition,

in recent years, Fe–S cofactored proteins have been found to also participate in DNA or RNA binding (Boal et al., 2005; Brown, 2005). Two common strategies to assess DNA or RNA binding are electrophoretic mobility shift assays (EMSA) and fluorescence anisotropy (FA). The application of these techniques for CPSF30/RNA binding is described later, and an example of these data are shown in Fig. 6.

6.1 Evaluation of CPSF30/RNA Binding via EMSA

In the EMSA assay, the RNA (or DNA) target is 5′ end labeled utilizing phosphate containing radioactively labeled ^{32}P, to allow determination of an interaction between protein and substrate (Fialcowitz-White et al., 2007; Hellman & Fried, 2007). In a typical experiment, the ^{32}P-RNA is incubated with increasing concentrations of protein, and the position of ^{32}P-RNA on the gel is shifted if binding occurs.

EMSA assays for CPSF30/RNA utilized α-synuclein pre-RNA; however, this assay can be adapted to examine any RNA sequence. An example of an EMSA assay for CPSF30 is shown in Fig. 6A.

Protocol

Radioactively labeling RNA

1. Quantitate RNA of interest as previously described (Section 2.1 step 40) and dilute to 5 pmol/μL using RNase-free water.
2. Add and mix the following reagents:

Reagent	Volume (μL)
5 μ*M* RNA	2
RNase-free water	4
10 × T4 PNK buffer (NEB Cat. No. B0201S)	1
[Υ^{32}P] ATP (6000 Ci/mmol stock)	2

3. Mix and then add 1 μL of T4 polynucleotide kinase to reach a final volume of 10 μL.
4. Incubate at 37°C for 10 min.
5. Add 50 μL of RNase-free water and 2 μL of 0.5 *M* EDTA.
6. Heat inactivate the reaction at 70°C for 15 min.
7. Extract once with 35 μL phenol: 35 μL of $CHCl_3$:IAA (chloroform: isoamyl alcohol) and mix by vortex.

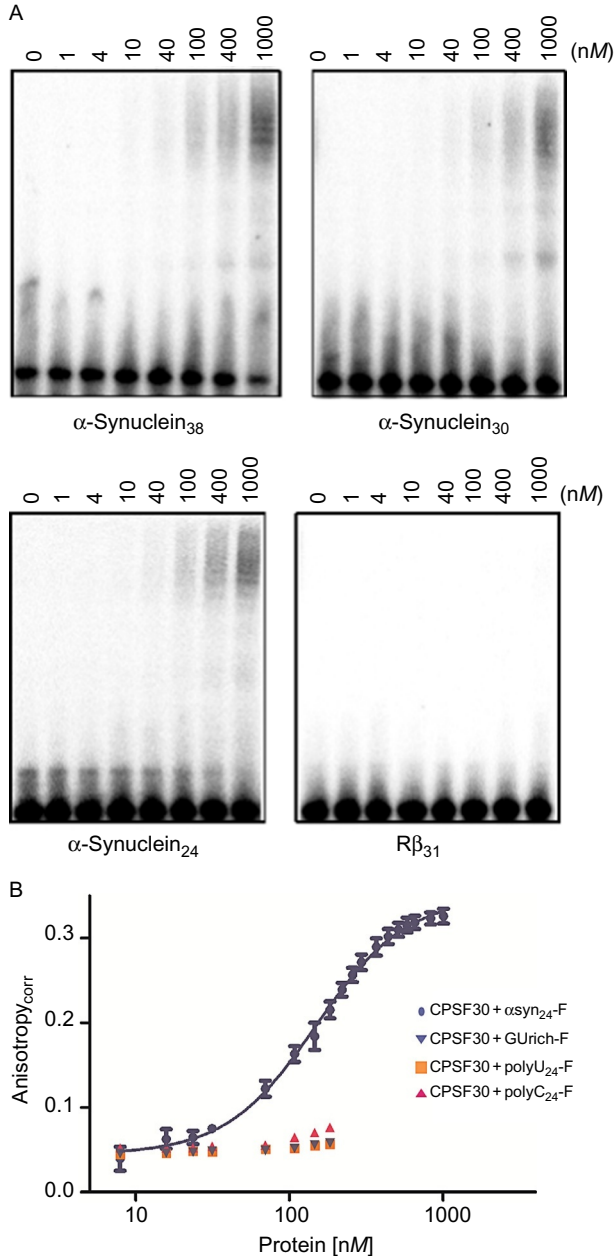

Fig. 6 Characterization of CPSF30/RNA binding. (A) EMSA data for CPSF30 with RNA (α-synuclein RNA sequence) at various sequence lengths, compared to a negative control with Rβ$_{31}$. (B) FA monitored titration of CPSF30 with α-synuclein RNA vs mutant RNA sequences. Binding is only observed with α-synuclein RNA, and these data are fit to a cooperative binding model with a $[P]_{1/2} = 143.8 \pm 3.8$ n*M* and a hill coefficient of 1.58 ± 0.07.

8. Remove unincorporated nucleotides by passage of the top aqueous layer through a G-25 spin column (Roche, Cat. No. 11273990001).
9. Quantify incorporation by liquid scintillation counting. Add 1 μL of RNA solution to 10 mL of scintillation fluid (Ecoscint H by National Diagnostics, Cat. No. LS-275) in a scintillation vial. This should yield between 2 and 3 K cpm/fmol.

   Note: The final concentration of RNA probes should be about 80 fmol/μL assuming 80% recovery in 100 μL of elution volume.

EMSA

Note: All water used must be RNase free and all reagents must be EDTA free.

1. Dilute the RNA probe to 2 n*M* using a 10-m*M* Tris, pH 8.0 buffer.
2. Prepare the following reaction mixture:

Reagent	Volume (μL)	Final Concentration
4 × LS-binding mix (400 m*M* Tris/800 m*M* KCl)	125	50 m*M* Tris pH 8.0 and 100 m*M* KCl
5 mg/mL poly-rC (Midland Certified Reagent Company, Cat. No. P-3002)	60	0.3 mg/mL
10 mg/mL acetylated BSA (Promega, Cat. No. R396D)	10	0.1 mg/mL
1.5 *M* DTT	1.6	2 m*M*
50% Glycerol	200	10% (v/v)
RNase-free water	590	N/A
10 m*M* $ZnCl_2$	10	100 μ*M*

3. Heat the RNA dilutions at 70°C for 5 min and then rest on ice for 3 min.
4. Incubate the ^{32}P-labeled RNA with increasing concentrations of CPSF30 (between 0 and 1000 n*M*) in the reaction mixture on ice for 15 min.

   Note: The final concentration of RNA probe in each assay should equal 0.2 n*M*.
5. Pipette the RNA or CPSF30/RNA mixture into lanes of a 5% (vol/vol) native polyacrylamide gel containing 10% (vol/vol) glycerol, with a 0.5 × (44.5 m*M*) Trisborate buffer (pH 8.0).

Note: The gel should be prerun at 150 V for 20 min before adding the RNA/CPSF30 mixture. During loading, run the gel at 80 V.

6. Run the gels at 200 V for approximately 3 h at 4°C.
7. Vacuum dry the gel for approximately 2 h (Bio-Rad model 583).
8. Expose the gel overnight using a phosphor screen.
9. Phosphorimage the gel next day (e.g., GE Typhoon FLA9500).

6.2 Quantification of ZF/RNA Binding via Fluorescence Anisotropy

Although EMSA can be utilized to quantify CPSF30/RNA binding (or other ZF/RNA binding), our laboratory uses FA. FA is a solution-based technique that measures the differences in polarization (anisotropy) that occur when a fluorescently labeled macromolecule binds to a non-fluorescently labeled macromolecule forming a complex (Lakowicz, 1999; Wilson, 2005). The FA measure is indirectly proportional to tumbling rate of the macromolecule, and when a complex forms, the tumbling rate decreases and an increase in FA is observed. A number of fluorophores can also be utilized. For the FA experiment with ZFs that bind RNA, we prefer to conjugate fluorescein to the 3′ end of our RNA, although 5′ end labeling can also be utilized. We excite at 495 n*M* and observe a maximum emission at 517 nm. An example of FA for CPSF30 with fluorescein-labeled RNA is shown in Fig. 6B and we describe our protocol below. The length of the target RNA sequence utilized should be optimized such that all regions of RNA involved in binding are present. For CPSF30, we find that RNA molecules between 24 and 38 nucleotides long are suitable for CPF30/RNA binding, and that our sequences do not appear to adopt any secondary structure (as measured by thermal denaturation). It should be noted that since FA readings are calculated from changes in apparent molecular size during binding, very large RNA sequences can attenuate measurements as the overall change in molecular size is lessened. FA is very versatile and can be adapted to any protein/DNA, protein/RNA, or protein/protein interaction of interest.

Protocol

1. *Fluorimeter schematics*. Experiments are conducted in the L format on an ISS PC-1 spectrofluorometer with polarizers. A full excitation/emission scan of F-labeled RNA to determine optimal excitation/emission wavelengths should be performed. We recommend an excitation wavelength/band pass of 495 nm/2 nm and an emission wavelength/bandpass of 517 nm/1 nm for fluorescein-labeled RNA.

2. Add 5 n*M* of fluorescently labeled RNA in 20 m*M* Tris, pH 7.0, 50 m*M* sodium chloride with 0.2 mg/mL BSA, and 0.4 mg/mL poly-rC to reach a final volume of 500 μL in a Spectrosil far UV quartz window fluorescence cuvette (Starna Cells). BSA serves to prevent protein adherence to the quartz cuvette walls and poly-rC is an internal negative control for nonspecific protein/RNA interactions.
3. Titrate the protein with the RNA and observe anisotropy changes until saturation. In a typical experiment, upon addition of the protein, the complex is incubated for 5 min. The protein is titrated in aliquots increasing concentrations beginning with 10 n*M*.

   Note: During the experiment, dilution of the sample should be taken into account and compensated for in a corrected anisotropy value that is calculated as follows:

$$\text{Corrected anisotropy} = \text{anisotropy} \times \frac{\text{starting reaction volume}}{\text{current volume}}$$

4. If some quenching of fluorescence is observed during the titration, the anisotropy (r) should be corrected for the change in quantum yield (Q, $f_{\text{free}}/f_{\text{bound}}$, protein-dependent change in fluorescence) using the following equation:

$$r_c = \frac{r_0(r_{\text{bound}} - r) + (r_{bound} Q(r - r_0))}{(r_{\text{bound}} - r + Q(r - r_0))}$$

   where r_c is the corrected anisotropy, r_0 is the anisotropy of the free fluorescein-labeled oligonucleotide, and r_{bound} is the anisotropy of the RNA–protein complex at saturation. Plot r_c against the concentration of protein.
5. Fit the data to an appropriate binding model. Our data were best fit to a cooperative binding model using nonlinear regression (GraphPad Prism 5):

$$nP + R \rightleftharpoons P_nR$$

$$K = \frac{[P_nR]}{[P]^n[R]}$$

$$r_{\mathrm{Tc}} = r_0 + (r_{\mathrm{bound}} - r_0)\left[\frac{\left(\frac{[\mathrm{P}]}{[\mathrm{P}]_{1/2}}^{h}\right)}{\left(1 + \left(\frac{[\mathrm{P}]}{[\mathrm{P}]_{1/2}}\right)^{h}\right)}\right]$$

r_{Tc} is the total, corrected anisotropy, r_0 is the anisotropy of the free fluorescein-labeled oligonucleotide, r_{bound} is the anisotropy of the RNA–protein complex at saturation, [P] is the concentration of protein, $[\mathrm{P}]_{1/2}$ is the concentration of protein at half-maximal saturation, and h is the Hill coefficient. (*Note*: it is always a best practice to fit data to several models, beginning with the simplest 1:1 binding).

7. CONCLUSIONS

A large number of proteins are annotated as ZF proteins in genome databases, but only a handful have been characterized experimentally. In Section 5, we described a general approach one can take to isolate a novel ZF protein, and evaluate which metal ions are present. We also present activity assays, EMSA and FA, that can be applied to identify whether the ZF binds to RNA or DNA.

ACKNOWLEDGMENTS

S.L.J.M. thanks the NSF for support of this work (CHE1708732, CHE1306208); G.D.S. has been partially supported by NIH training Grant T32GM066706-13. We thank Dr. Tim Stemmler (Wayne State) and Dr. Gerald Wilson (Maryland School of Medicine), for their fantastic collaborations.

REFERENCES

Adrover, M., Howes, B. D., Iannuzzi, C., Smulevich, G., & Pastore, A. (2015). Anatomy of an iron-sulfur cluster scaffold protein: Understanding the determinants of [2Fe-2S] cluster stability on IscU. *Biochimica et Biophysica Acta*, *1853*(6), 1448–1456. https://doi.org/10.1016/j.bbamcr.2014.10.023.

AKTA pure: User Manual. (2012). *General Electric*.

Andreini, C., Banci, L., Bertini, I., & Rosato, A. (2006). Zinc through the three domains of life. *Journal of Proteome Research*, *5*(11), 3173–3178. https://doi.org/10.1021/pr0603699.

Barbas, C. F., 3rd, Burton, D. R., Scott, J. K., & Silverman, G. J. (2007). Quantitation of DNA and RNA. *CSH Protocols* pdb ip47https://doi.org/10.1101/pdb.ip47.

Baxter, E. L., Jennings, P. A., & Onuchic, J. N. (2012). Strand swapping regulates the iron-sulfur cluster in the diabetes drug target mitoNEET. *Proceedings of the National Academy of Sciences of the United States of America*, *109*(6), 1955–1960. https://doi.org/10.1073/pnas.1116369109.

Beaudoing, E., Freir, S., Wyatt, J. R., Claverie, J. M., & Gautheret, D. (2000). Patterns of variant polyadnylation signal usage in human genes. *Genome Research*, *10*(7), 1001–1010.

Berg, J. M. (1986). Potential metal-binding domains in nucleic acid binding proteins. *Science*, *232*(4749), 485–487.

Berg, J. M. (1988). Proposed structure for the zinc-binding domains from transcription factor IIIA and related proteins. *Proceedings of the National Academy of Sciences of the United States of America*, *85*(1), 99–102.

Bertani, G. (1951). A method for detection of mutations, using streptomycin dependence in *Escherichia coli*. *Genetics*, *36*(6), 598–611.

Bertini, I., Decaria, L., & Rosato, A. (2010). The annotation of full zinc proteomes. *Journal of Biological Inorganic Chemistry*, *15*(7), 1071–1078. https://doi.org/10.1007/s00775-010-0666-6.

Biolabs, N. E. (2015). *PCR protocol for* Taq *DNA polymerase with standard Taq buffer (M0273)*.

Blanc, B., Gerez, C., & Ollagnier de Choudens, S. (2015). Assembly of Fe/S proteins in bacterial systems: Biochemistry of the bacterial ISC system. *Biochimica et Biophysica Acta*, *1853*(6), 1436–1447. https://doi.org/10.1016/j.bbamcr.2014.12.009.

Boal, A. K., Yavin, E., Lukianova, O. A., O'Shea, V. L., David, S. S., & Barton, J. K. (2005). DNA-bound redox activity of DNA repair glycosylases containing [4Fe-4S] clusters. *Biochemistry*, *44*(23), 8397–8407. https://doi.org/10.1021/bi047494n.

Boon, E. M., Livingston, A. L., Chmiel, N. H., David, S. S., & Barton, J. K. (2003). DNA-mediated charge transport for DNA repair. *Proceedings of the National Academy of Sciences of the United States of America*, *100*(22), 12543–12547. https://doi.org/10.1073/pnas.2035257100.

Brown, R. S. (2005). Zinc finger proteins: Getting a grip on RNA. *Current Opinion in Structural Biology*, *15*(1), 94–98. https://doi.org/10.1016/j.sbi.2005.01.006.

Chmiel, N. H., Golinelli, M. P., Francis, A. W., & David, S. S. (2001). Efficient recognition of substrates and substrate analogs by the adenine glycosylase MutY requires the C-terminal domain. *Nucleic Acids Research*, *29*(2), 553–564.

Colca, J. R., McDonald, W. G., Waldon, D. J., Leone, J. W., Lull, J. M., Bannow, C. A., et al. (2004). Identification of a novel mitochondrial protein ("mitoNEET") cross-linked specifically by a thiazolidinedione photoprobe. *American Journal of Physiology Endocrinology and Mebatolism*, *286*, E252–E260.

Conlan, A. R., Axelrod, H. L., Cohen, A. E., Abresch, E. C., Zuris, J., Yee, D., et al. (2009). Crystal structure of Miner1: The redox-active 2Fe-2S protein causative in Wolfram Syndrome 2. *Journal of Molecular Biology*, *392*(1), 143–153. https://doi.org/10.1016/j.jmb.2009.06.079.

Dailey, H. A., Finnegan, M. G., & Johnson, M. K. (1994). Human ferrochelatase is an iron-sulfur protein. *Biochemistry*, *33*(2), 403–407.

Decaria, L., Bertini, I., & Williams, R. J. (2010). Zinc proteomes, phylogenetics and evolution. *Metallomics*, *2*(10), 706–709. https://doi.org/10.1039/c0mt00024h.

Engstrom, L. M., Partington, O. A., & David, S. S. (2012). An iron-sulfur cluster loop motif in the Archaeoglobus fulgidus uracil-DNA glycosylase mediates efficient uracil recognition and removal. *Biochemistry*, *51*(25), 5187–5197. https://doi.org/10.1021/bi3000462.

Feliu, J. X., Cubarsi, R., & Villaverde, A. (1998). Optimized release of recombinant proteins by ultrasonication of E. coli cells. *Biotechnology and Bioengineering*, *58*(5), 536–540.

Fialcowitz-White, E. J., Brewer, B. Y., Ballin, J. D., Willis, C. D., Toth, E. A., & Wilson, G. M. (2007). Specific protein domains mediate cooperative assembly of HuR oligomers on AU-rich mRNA-destabilizing sequences. *The Journal of Biological Chemistry*, *282*(29), 20948–20959. https://doi.org/10.1074/jbc.M701751200.

Gel Filtration Molecular Weight Markers Kit for Molecular Weights 12,000–200,000 Da Technical Bulletin. n.d. Sigma-Aldrich.

Hellman, L. M., & Fried, M. G. (2007). Electrophoretic mobility shift assay (EMSA) for detecting protein-nucleic acid interactions. *Nature Protocols*, *2*(8), 1849–1861. https://doi.org/10.1038/nprot.2007.249.

Ho, C. W., Chew, T. K., Ling, T. C., Kamaruddin, S., Tan, W. S., & Tey, B. T. (2006). Efficient mechanical cell disruption of Escherichia coli by an ultrasonicator and recovery of intracellular hepatitis B core antigen. *Process Biochemistry*, *41*(8), 1829–1834. https://doi.org/10.1016/j.procbio.2006.03.043.

Jaganaman, S., Pinto, A., Tarasev, M., & Ballou, D. P. (2007). High levels of expression of the iron-sulfur proteins phthalate dioxygenase and phthalatedioxygenase reductase in Escherichia coli. *Protein Expression and Purification*, *52*(2), 273–279.

Jantz, D., Amann, B. T., Gatto, G. J., Jr., & Berg, J. M. (2004). The design of functional DNA-binding proteins based on zinc finger domains. *Chemical Reviews*, *104*(2), 789–799. https://doi.org/10.1021/cr020603o.

Kapust, R. B., & Waugh, D. S. (1999). Escherichia coli maltose-binding protein is uncommonly effective at promoting the solubility of polypeptides to which it is fused. *Protein Science*, *8*(8), 1668–1674. https://doi.org/10.1110/ps.8.8.1668.

Krishna, S. S., Majumdar, I., & Grishin, N. V. (2003). Structural classification of zinc fingers: Survey and summary. *Nucleic Acids Research*, *31*(2), 532–550.

Kurz, M., Cowieson, N. P., Robin, G., Hume, D. A., Martin, J. L., Kobe, B., et al. (2006). Incorporating a TEV cleavage site reduces the solubility of nine recombinant mouse proteins. *Protein Expression and Purification*, *50*(1), 68–73. https://doi.org/10.1016/j.pep.2006.05.006.

Laity, J. H., Lee, B. M., & Wright, P. E. (2001). Zinc finger proteins: New insights into structural and functional diversity. *Current Opinion in Structural Biology*, *11*(1), 39–46.

Lakowicz, J. R. (1999). Fluorescence anisotropy. In *Principles of fluorescence spectroscopy* (pp. 291–319). United States: Springer.

Lanz, N. D., Grove, T. L., Gogonea, C. B., Lee, K. H., Krebs, C., & Booker, S. J. (2012). RlmN and AtsB as models for the overproduction and characterization of radical SAM proteins. *Methods in Enzymology*, *516*, 125–152. https://doi.org/10.1016/B978-0-12-394291-3.00030-7.

Larentis, A. L., Nicolau, J. F., Esteves Gdos, S., Vareschini, D. T., de Almeida, F. V., dos Reis, M. G., et al. (2014). Evaluation of pre-induction temperature, cell growth at induction and IPTG concentration on the expression of a leptospiral protein in E. coli using shaking flasks and microbioreactor. *BMC Research Notes*, 7, 671. https://doi.org/10.1186/1756-0500-7-671.

Lee, B. M., De Guzman, R. N., Turner, B. G., Tjandra, N., & Summers, M. F. (1998). Dynamical behavior of the HIV-1 nucleocapsid protein. *Journal of Molecular Biology*, *279*(3), 633–649. https://doi.org/10.1006/jmbi.1998.1766.

Lee, S. J., & Michel, S. L. (2014). Structural metal sites in nonclassical zinc finger proteins involved in transcriptional and translational regulation. *Accounts of Chemical Research*, *47*(8), 2643–2650. https://doi.org/10.1021/ar500182d.

Lee, K.-H., Saleh, L., Anton, B. P., Madinger, C. L., Benner, J. S., Iwig, D. F., et al. (2009). Characterization of RimO, a new member of the methylthiotransferase subclass of the radical SAM superfamily. *Biochemistry*, *48*(42), 10162–10174. https://doi.org/10.1021/bi900939w.

Li, H., Mapolelo, D. T., Dingra, N. N., Naik, S. G., Lees, N. S., Hoffman, B. M., et al. (2009). The yeast iron regulatory proteins Grx3/4 and Fra2 form heterodimeric complexes containing a [2Fe-2S] cluster with cysteinyl and histidyl ligation. *Biochemistry*, *48*(40), 9569–9581. https://doi.org/10.1021/bi901182w.

Lin, J., Zhang, L., Lai, S., & Ye, K. (2011). Structure and molecular evolution of CDGSH iron-sulfur domains. *PLoS One*, *6*(9), e24790. https://doi.org/10.1371/journal.pone.0024790.

Lipper, C. H., Paddock, M. L., Onuchic, J. N., Mittler, R., Nechushtai, R., & Jennings, P. A. (2015). Cancer-related NEET porteins transfer 2Fe-2S clusters to Anamorsin, a protein required for cytosolic iron-sulfur cluster biogenesis. *PLoS One*, *10*(10), e0139699, https://doi.org/10.1371/journal.pone.0139699.

Liu, Q., Xia, Z., & Case, C. C. (2002). Validated zinc finger protein designs for All 16 GNN DNA triplet targets. *The Journal of Biological Chemistry*, *277*(6), 3850–3856. https://doi.org/10.1074/jbc.M110669200.

Magyar, J. S., & Godwin, H. A. (2003). Spectropotentiometric analysis of metal binding to structural zinc-binding sites: Accounting quantitatively for pH and metal ion buffering effects. *Analytical Biochemistry*, *320*(1), 39–54.

Mapolelo, D. T., Zhang, B., Naik, S. G., Huynh, B. H., & Johnson, M. K. (2012). Spectroscopic and functional characterization of iron-sulfur cluster-bound forms of Azotobacter vinelandii (Nif)IscA. *Biochemistry*, *51*(41), 8071–8084. https://doi.org/10.1021/bi3006658.

Maret, W. (2012). New perspectives of zinc coordination environments in proteins. *Journal of Inorganic Biochemistry*, *111*, 110–116. https://doi.org/10.1016/j.jinorgbio.2011.11.018.

Matthews, J. M., & Sunde, M. (2002). Zinc fingers—Folds for many occasions. *IUBMB Life*, *54*(6), 351–355. https://doi.org/10.1080/15216540216035.

McCurdy, E., Woods, G., & Potter, D. (2006). *Unmatched removal of spectral interferences in ICP-MS using the agilent octopole reaction system with helium collision mode*. Agilent Technologies.

Michalek, J. L., Besold, A. N., & Michel, S. L. (2011). Cysteine and histidine shuffling: Mixing and matching cysteine and histidine residues in zinc finger proteins to afford different folds and function. *Dalton Transactions*, *40*(47), 12619–12632. https://doi.org/10.1039/c1dt11071c.

Miller, J., McLachlan, A. D., & Klug, A. (1985). Repetitive zinc-binding domains in the protein transcription factor IIIA from Xenopus oocytes. *EMBO Journal*, *4*(6), 1609–1614.

Newton, A., Mackay, J., & Crossley, M. (2001). The N-terminal zinc finger of the erythroid transcription factor GATA-1 binds GATC motifs in DNA. *The Journal of Biological Chemistry*, *276*(38), 35794–35801. https://doi.org/10.1074/jbc.M106256200.

Pattenden, L. K., & Thomas, W. G. (2008). Amylose affinity chromatography of maltose-binding protein: Purification by both native and novel matrix-assisted dialysis refolding methods. *Methods in Molecular Biology*, *421*, 169–189.

Pavletich, N. P., & Pabo, C. O. (1991). Zinc finger-DNA recognition: Crystal structure of a Zif268-DNA complex at 2.1 Å. *Science*, *252*(5007), 809–817.

Persikov, A. V., & Singh, M. (2014). De novo prediction of DNA-binding specificities for Cys2His2 zinc finger proteins. *Nucleic Acids Research*, *42*(1), 97–108. https://doi.org/10.1093/nar/gkt890.

Phan, J., Zdanov, A., Evdokimov, A. G., Tropea, J. E., Peters, H. K., Kapust, R. B., et al. (2002). Structural basis for the substrate specificity of tobacco etch virus protease. *The Journal of Biological Chemistry*, *277*(52), 50564–50572. https://doi.org/10.1074/jbc.M207224200.

Poor, C. B., Wegner, S. V., Li, H., Dlouhy, A. C., Schuermann, J. P., Sanishvili, R., et al. (2014). Molecular mechanism and structure of the Saccharomyces cerevisiae iron regulator Aft2. *Proceedings of the National Academy of Sciences of the United States of America*, *111*(11), 4043–4048. https://doi.org/10.1073/pnas.1318869111.

Profrock, D., & Prange, A. (2012). Inductively coupled plasma-mass spectrometry (ICP-MS) for quantitative analysis in environmental and life sciences: A review of challenges, solutions, and trends. *Applied Spectroscopy*, *66*(8), 843–868. https://doi.org/10.1366/12-06681.

Rommers, P., & Boumans, P. (1996). ICP-AES versus (LA-)IPC-MS: Competition or a happy marriage? A view supported by current data. *Fresenius Journal of Analytical Chemistry*, *355*(7–8), 763–770.

Rosano, G. L., & Ceccarelli, E. A. (2014). Recombinant protein expression in microbial systems. *Frontiers in Microbiology*, *5*, 341. https://doi.org/10.3389/fmicb.2014.00341.

Segura, M., Madrid, Y., & Cámara, C. (2003). Elimination of calcium and argon interferences in iron determination by ICP-MS using desferrioxamine chelating agent

immobilized in sol–gel and cold plasma conditions. *Journal of Analytical Atomic Spectrometry*, *18*(9), 1103–1108. https://doi.org/10.1039/B301719M.

Shimberg, G. D., Michalek, J. L., Oluyadi, A. A., Rodrigues, A. V., Zucconi, B. E., Neu, H. M., et al. (2016). Cleavage and polyadenylation specificity factor 30: An RNA-binding zinc-finger protein with an unexpected 2Fe-2S cluster. *Proceedings of the National Academy of Sciences of the United States of America*, *113*(17), 4700–4705. https://doi.org/10.1073/pnas.1517620113.

Simonian, M. H., & Smith, J. A. (2006). Spectrophotometric and colorimetric determination of protein concentration. *Current Protocols in Molecular Biology* chapter 10, Unit 10 11A, 10.1.1–10.1A.9https://doi.org/10.1002/0471142727.mb1001as76.

Smith, B. (1994). Drying gels. In J. Walker (Ed.), *Basic protein and peptide protocols* (pp. 157–161). Humana Press.

Tamir, S., Paddock, M. L., Darash-Yahana-Baram, M., Holt, S. H., Sohn, Y. S., Agranat, L., et al. (2015). Structure-function analysis of NEET proteins uncovers their role as key regulators of iron and ROS homeostasis in health and disease. *Biochimica et Biophysica Acta*, *1853*(6), 1294–1315. https://doi.org/10.1016/j.bbamcr.2014.10.014.

Tan, G., Landry, A. P., Dai, R., Wang, L., Lu, J., & Ding, H. (2012). Competition of zinc ion for the [2Fe-2S] cluster binding site in the diabetes drug target protein mitoNEET. *Biometals*, *25*(6), 1177–1184. https://doi.org/10.1007/s10534-012-9580-4.

Vandevenne, M., Jacques, D. A., Artuz, C., Nguyen, C. D., Kwan, A. H., Segal, D. J., et al. (2013). New insights into DNA recognition by zinc fingers revealed by structural analysis of the oncoprotein ZNF217. *The Journal of Biological Chemistry*, *288*(15), 10616–10627. https://doi.org/10.1074/jbc.M112.441451.

Wang, Y., Landry, A. P., & Ding, H. (2017). The mitochondrial outer membrane protein mitoNEET is a redox enzyme catalyzing electron transfer from FMNH2 to oxygen or ubiqunone. *The Journal of Biological Chemistry*, *292*(24), 10061–10067. https://doi.org/10.1074/jbc.M117.789800Epub 2017 May 1.

Warf, M. B., & Berglund, J. A. (2007). MBNL binds similar RNA structures in the CUG repeats of myotonic dystrophy and its pre-mRNA substrate cardiac troponin T. *RNA*, *13*(12), 2238–2251. https://doi.org/10.1261/rna.610607.

Wiley, S. E., Murphy, A. N., Ross, S. A., van der Geer, P., & Dixon, J. E. (2007). MitoNEET is an iron-containing outer mitochondrial membrane protein that regulates oxidative capacity. *Proceedings of the National Academy of Sciences of the United States of America*, *104*(13), 5318–5323. https://doi.org/10.1073/pnas.0701078104.

Wiley, S. E., Paddock, M. L., Abresch, E. C., Gross, L., van der Geer, P., Nechushtai, R., et al. (2007). The outer mitochondrial membrane protein mitoNEET contains a novel redox-active 2Fe-2S cluster. *The Journal of Biological Chemistry*, *282*(33), 23745–23749. https://doi.org/10.1074/jbc.C700107200.

Wilson, G. M. (2005). RNA folding and RNA-protein binding analyzed by fluorescence anisotropy and resonance engery transfer. In C. D. Geddes & J. R. Lakowicz (Eds.), *Reviews in fluorescence*, Vol. 2 (p. 20). New York: Springer Science + Business Media, Inc.

Woestenenk, E. A., Hammarström, M., van den Berg, S., Härd, T., & Berglund, H. (2004). His tag effect on solubility of human proteins produced in Escherichia coli: A comparison between four expression vectors. *Journal of Structural and Functional Genomics*, *5*(3), 217–229. https://doi.org/10.1023/B:jsfg.0000031965.37625.0e.

Yang, Q., & Doublie, S. (2011). Structural biology of poly(A) site definition. *Wiley Interdisciplinary Reviews RNA*, *2*(5), 732–747. https://doi.org/10.1002/wrna.88.

Zhao, D., & Huang, Z. (2016). Effect of His-Tag on expression, purification and structure of zinc finger protein, ZNF191(243-368). *Bioinorganic Chemistry and Applications 2016*, 8206854. https://doi.org/10.1155/2016/8206854.

Zoorob, G. K., McKiernan, J. W., & Caruso, J. A. (1998). ICP-MS for elemental speciation studies. *Mikrochimica Acta*, *128*(3–4), 145–168. https://doi.org/10.1007/Bf01243044.